



Contents lists available at ScienceDirect

Biomaterials

journal homepage: www.elsevier.com/locate/biomaterials

Regulation of the endothelialization by human vascular endothelial cells by ZNF580 gene complexed with biodegradable microparticles

Changcan Shi^a, Fanglian Yao^{a,b,c}, Qian Li^a, Musammir Khan^a, Xiangkui Ren^a, Yakai Feng^{a,b,c,d,*}, Jiawen Huang^e, Wencheng Zhang^{f,**}

^aSchool of Chemical Engineering and Technology, Tianjin University, Tianjin 300072, China

^bKey Laboratory of Systems Bioengineering of Ministry of Education, Tianjin University, Tianjin 300072, China

^cTianjin University-Helmholtz-Zentrum Geesthacht, Joint Laboratory for Biomaterials and Regenerative Medicine, Tianjin 300072, China

^dCollaborative Innovation Center of Chemical Science and Chemical Engineering (Tianjin), Tianjin 300072, China

^eGraduate School of Tianjin Medical University, Tianjin 300070, China

^fDepartment of Physiology and Pathophysiology, Logistics University of Chinese People's Armed Police Force, Tianjin 300162, China

ARTICLE INFO

Article history:

Received 6 April 2014

Accepted 28 April 2014

Available online xxx

Keywords:

Triblock copolymers

Microparticles

Biodegradable

Non-viral gene carrier

ZNF580 gene

Rapid endothelialization

ABSTRACT

The lack of living endothelial cells (ECs) functional layer is one of the major reasons which account for thrombosis of synthetic vascular vessels. To overcome this obstacle, we employed ZNF580 gene complexed with biodegradable microparticles (MPs) to promote the rapid endothelialization by ECs. In order to realize the controlled release of ZNF580 gene from MPs/gene complexes, a series of amphiphilic triblock copolymers with different degradation rate, namely, methoxy-poly(ethylene glycol)-block-poly(3(S)-methyl-morpholine-2,5-dione)-graft-polyethyleneimine (mPEG-b-PMMD-g-PEI), methoxy-poly(ethylene glycol)-block-poly(3(S)-methyl-morpholine-2,5-dione-co-lactide)-graft-polyethyleneimine (mPEG-b-P(MMD-co-LA)-g-PEI) and methoxy-poly(ethylene glycol)-block-poly(3(S)-methyl-morpholine-2,5-dione-co-lactide-co-glycolide)-graft-polyethyleneimine (mPEG-b-P(MMD-co-LA-co-GA)-g-PEI), were synthesized. Then, MPs were formed by self-assembly. The hydrophobic cores of these MPs were composed of PMMD, P(MMD-LA) or P(MMD-co-LA-co-GA) segments, and provided crosslinking points for numbers of PEG and short PEI chains to form a high hydrophilic and positive charged corona/shell structure.

Based on their positive charged surface, MPs can compact pEGFP-ZNF580 into MPs/pEGFP-ZNF580 complexes. The cell transfection result demonstrated that pEGFP-ZNF580 could be transported efficiently into ECs by these complexes. The result of western blot showed that the relative ZNF580 protein level can increase to 35.74%–46.11% by the overexpression of ZNF580 gene. Furthermore, the release of pEGFP-ZNF580 could be sustained at least 25 days due to the controllable degradation ability of the hydrophobic MPs' core. The MPs and MPs/pEGFP-ZNF580 complexes showed low cytotoxicity because of the introduction of PEG chains and low molecular weight PEI on the surface of these MPs. Notably, at the low concentration (20 µg/mL), the MPs and their complexes were non-cytotoxicity. The rapid endothelialization was promoted significantly by the expression of pEGFP-ZNF580.

© 2014 Elsevier Ltd. All rights reserved.

1. Introduction

The age-standardized cardiovascular diseases have greatly increased in low- and middle-income countries in recently

decades, and become one of the major causes of death in China. In the treatment of occluded coronary arteries, coronary bypass surgery is one of the most important procedures. However, during the clinical application of artificial blood vessels, thrombosis, intimal hyperplasia and low long-term patency rate encountered, because of the hydrophobicity and the lack of living endothelial cells (ECs) functional layer on the artificial blood vessels' inner surface [1]. To increase the hydrophilic of the artificial blood vessels, surface modification was employed by many researchers [2] and our research group [3–7].

* Corresponding author. School of Chemical Engineering and Technology, Tianjin University, Tianjin 300072, China.

** Corresponding author.

E-mail addresses: yakaifeng@tju.edu.cn, yakaifeng@hotmail.com (Y. Feng), wenchengzhang@yahoo.com (W. Zhang).

A lot of methods have been explored to form an ECs functional layer on the inner surface of artificial blood vessels. For example, ECs seeded grafts were explored to get a reasonable patency rates by employing the ability of ECs to inhibit the full range of the vascular response to injury. Recently, it was found that the attachment of ECs and the rapid endothelialization on the stent could be enriched and accelerated by the anti-CD34 antibody [8], and ECs regeneration could be improved by aminolysis and biomacromolecule immobilization on the polyurethane scaffolds [9].

As an important growth factor, vascular endothelial growth factor (VEGF) has been widely used to increase the endothelialization on the artificial blood vessel surface with many methods [10]. For example, in order to enhance the ECs proliferation, VEGF and platelet-derived growth factor-bb (PDGF) were used in the dual-delivery function electrospun membranes [11]. Besides VEGF, a potential gene (ZNF580) for specific cellular proliferation has been studied for many years. It was found previously that the expression of ZNF580 gene could be up-regulated by H_2O_2 via the NF- κ B signaling pathway [12]. More importantly, ZNF580 gene plays an important role in the intervention of atherosclerosis and the process of migration and proliferation of ECs [13]. Notably, compared with VEGF, ZNF580 gene not only promotes the proliferation of ECs, but also inhibits the proliferation of smooth muscles. Although ZNF580 gene has been proved to possess huge advantage in rapid endothelialization *in vitro* [13], to the best of our knowledge, the application of ZNF580 gene in the artificial blood vessel remains unexplored.

Gene therapy has been used to treat and cure numbers of acquired diseases, therefore, the development of safe and effective gene carrier is of great importance for gene therapy. Polycations, such as polyethylenimine (PEI), polyamidoamine and chitosan have been reported to deliver nucleic acids [14]. Compared with viral carriers and cationic lipids, as the major type of non-viral gene delivery carrier, polycations show low host immunogenicity, and can be synthesized on a large scale.

As the “golden” standard for gene delivery, PEI is the most effective non-viral gene carriers *in vitro* and *in vivo* because of its unique combination of high charge density and enhanced “proton sponge effect” in endolysosomes [15]. Nevertheless, PEI is non-degradable, furthermore, it is known that the high degree of toxicity of PEI to cells was caused by its membrane disruptive properties [16].

Low molecular weight PEI ($M_w < 2000$) generally exhibits much lower toxicity, but its transfection is inefficient [17]. In order to increase its transfection, many effects have been done [18]. However, the lack of gene carriers with low toxicity, high transfection efficiency and controlled release properties remains a long-lasting challenge. Therefore, it is necessary to develop a gene delivery system to overcome this obstacle. In addition, it is of great interest to know whether it is possible to encapsulate ZNF580 gene into a delivery system to form a microparticle/gene complex to promote the rapid endothelialization by ECs.

The purpose of the present study is to develop biodegradable and low cytotoxic gene carriers. We synthesized a series triblock copolymers of methoxy-poly(ethylene glycol)-block-poly(3(S)-methyl-morpholine-2,5-dione-graft-polyethyleneimine (mPEG-b-PMMD-g-PEI), methoxy-poly(ethylene glycol)-block-poly(3(S)-methyl-morpholine-2,5-dione-co-lactide)-graft-polyethyleneimine (mPEG-b-P(MMD-co-LA)-g-PEI) and methoxy-poly(ethylene glycol)-block-poly(3(S)-methyl-morpholine-2,5-dione-co-lactide-co-glycolide)-graft-polyethyleneimine (mPEG-b-P(MMD-co-LA-co-GA)-g-PEI).

As the non-viral gene carriers, three kinds of microparticles (MPs) with different hydrophobic cores were obtained by self-assembly of these copolymers. The cores of these MPs were

composed by the PMMD, P(MMD-co-LA) or P(MMD-co-LA-co-GA) segments. They were synthesized from lactide (LA), glycolide (GA) and 3(S)-methyl-morpholine-2,5-dione (MMD) since they are commonly used monomers for the synthesis of non-toxic and biodegradable biomaterials. Herein, mPEG is used as hydrophilic constituent [19], while PEI ($M_w = 1800$) was used to prepare the carrier for its low toxicity despite of its low transfection efficiency. So, numbers of PEG as the hydrophilic corona and short PEI chains as the cationic shell were connected with the core.

To improve the transfection capacity, many amphiphilic copolymer molecules were controlled to assemble and form a micro-particle with considerable positive charges. MPs/pEGFP-ZNF580 complexes with different positive charges were formed by adjusting N/P molar ratios. Based on the MPs/pEGFP-ZNF580 complexes, pEGFP-ZNF580 can be delivered into ECs and expressed after release.

2. Materials and methods

2.1. Materials

3-(4,5-Dimethylthiazol-2-yl)-2,5-diphenyltetrazolium bromide (MTT), polyethylenimine (branched PEI, $M_w = 1800$), mPEG ($M_w = 5000$) and stannous octoate were purchased from Sigma–Aldrich (St. Louis, USA). L-Lactide (L-LA) and GA were obtained from Foryou Medical Device Co., Ltd. (Huizhou, China). L-Alanine and chloroacetyl chloride were supplied by Aladdin Reagent Co., Ltd. (Shanghai, China). Dimethyl sulphoxide (DMSO) was purchased from Sigma (St. Louis, MO). Lipofectamine™ 2000 reagent was purchased from Invitrogen (Grand Island, USA). BCA protein assay kit was purchased from Solarbio Science and Technology Co., Ltd. (Beijing, China). Rabbit Anti-human ZNF580 polyclonal antibody and goat anti-rabbit Ig G were purchased from Abcam (HK) Ltd. (Hong Kong, China). The pEGFP-ZNF580 was preserved by department of physiology and pathophysiology, logistics university of Chinese People's Armed Police Force. MMD monomer was prepared using our previously reported method [20].

2.2. Synthesis of amphiphilic triblock copolymers

2.2.1. Diblock copolymers

Diblock copolymers of mPEG-b-PMMD, mPEG-b-P(MMD-co-LA) and mPEG-b-P(MMD-co-LA-co-GA) were prepared by ring-opening polymerization (ROP) of relative monomers [21]. The synthesis process was illustrated by the example of mPEG-b-PMMD. Briefly, mPEG (1.65 g, $M_w = 5000$), MMD (2.31 g) and Sn(Oct)₂ toluene solution (200 μ L, 2.9%) were added in a flame-dried and nitrogen-purged flask (10 mL). The flask was sealed and maintained at 155 °C for 12 h. The copolymer was recovered by dissolving in DMSO and followed by precipitation in ice-cold ether. The resultant precipitate (mPEG-b-PMMD) was filtered and dried at room temperature in vacuum until constant weight. In addition, mPEG-b-P(MMD-co-LA) and mPEG-b-P(MMD-co-LA-co-GA) copolymers were synthesized by the analogous method.

2.2.2. Amphiphilic triblock copolymers

Amphiphilic triblock copolymers were synthesized by grafting PEI onto diblock copolymers. The amphiphilic triblock copolymers were named as mPEG-b-PMMD-g-PEI, mPEG-b-P(MMD-co-LA)-g-PEI and mPEG-b-P(MMD-co-LA-co-GA)-g-PEI, indicating that they were prepared from mPEG-b-PMMD, mPEG-b-P(MMD-co-LA) or mPEG-b-P(MMD-co-LA-co-GA) and PEI, respectively.

The synthesis process was illustrated by the example of mPEG-b-PMMD-g-PEI. Briefly, mPEG-b-PMMD diblock copolymer (1.0 g) was dissolved in DMSO (9.5 mL), and then the solution was transferred into a dried constant pressure funnel (25 mL). Dibutyl tin dilaurate (DBTDL, 10 μ L) and isophorone diisocyanate (IPDI) toluene solution (319 μ L, 1%) were added in a three-necked flask (50 mL). mPEG-b-PMMD solution was added dropwise into the flask under stirring at 30 °C in 30 min, and then reacted for 24 h. The reaction mixture was added dropwise into 2.62 mL of PEI toluene solution (10%) under a nitrogen atmosphere at 60 °C in 3 h, and then reacted for 24 h. When the solution was cooled to room temperature, triblock copolymer (mPEG-b-PMMD-g-PEI) was obtained by precipitation in ice-cold ether as white flocculent precipitate. The resultant precipitate was filtered and dried at room temperature in vacuum until constant weight. With the analogous method, mPEG-b-P(MMD-co-LA)-g-PEI and mPEG-b-P(MMD-co-LA-co-GA)-g-PEI copolymers were synthesized.

2.3. Characterization of copolymers

FT-IR spectra of the copolymers were obtained using an FT-IR spectrometer (Bio-Rad FTS-6000, USA). Moreover, ¹H NMR spectra of the copolymers were recorded with a Bruker Avance spectrometer (AV-400, Bruker, Karlsruhe, Germany) operating at 400 MHz in CDCl₃ or DMSO-d₆. The average molecular weight (M_w) was

determined by gel permeation chromatography (GPC, Malvern Viscotek, UK) with tetrahydrofuran (THF) as elute.

2.4. Biodegradation of the copolymers

To study the degradation behavior of the copolymers *in vitro*, biodegradation test was employed as reported previously [22]. The molded samples were cut into a rectangular shape with dimensions of $10 \times 10 \times 0.2 \text{ mm}^3$ and placed in closed bottles containing 80 mL of PBS (pH = 7.4), the bottles were incubated in air bath shaker (50 rpm) at 37 °C for 50 days. The PBS was exchanged every 5 days, at different time interval the samples were washed with distilled water and dried at room temperature in vacuum until constant weight. Then, they were weighted to obtain the W_t . The degradation rates were estimated by the percentage of weight loss. The residual weight (%) of the copolymers was calculated using the following formula: (W_0 : the original weight of the copolymer sample; W_t : the sample weight at different time interval):

$$\text{Residual weight (\%)} = \frac{W_t}{W_0} \times 100\%$$

2.5. Critical micelle concentration (CMC)

The CMC of triblock copolymers were determined using pyrene as an extrinsic probe [21,23]. 12.4 mg of pyrene was dissolved in acetone (1000 mL); the final concentration of the solution (A) was $6 \times 10^{-5} \text{ mol/L}$. 100 mg of polymer was dissolved in 10 mL triple-distilled water, the final concentration of copolymer solution is 10 mg/mL. Then, a series of different concentrations from 10^{-6} mg/mL to 10 mg/mL of polymer solution (B) were prepared from the 10 mg/mL copolymer solution. 40 μL of solution (A) were transferred into a tube and evaporated with N_2 , 4 mL of solution (B) were added to the tube, and the final concentration of pyrene solution was $6 \times 10^{-7} \text{ mol/L}$.

Steady-state fluorescence spectra were obtained with Cary Eclipse fluorescence spectrometer. The ratios of excitation spectral intensities at 338 nm and 333 nm (I_{338}/I_{333}) were calculated and plotted against the logarithm of polymer mass concentration.

2.6. Preparation and characterization of MPs/pEGFP-ZNF580 complexes

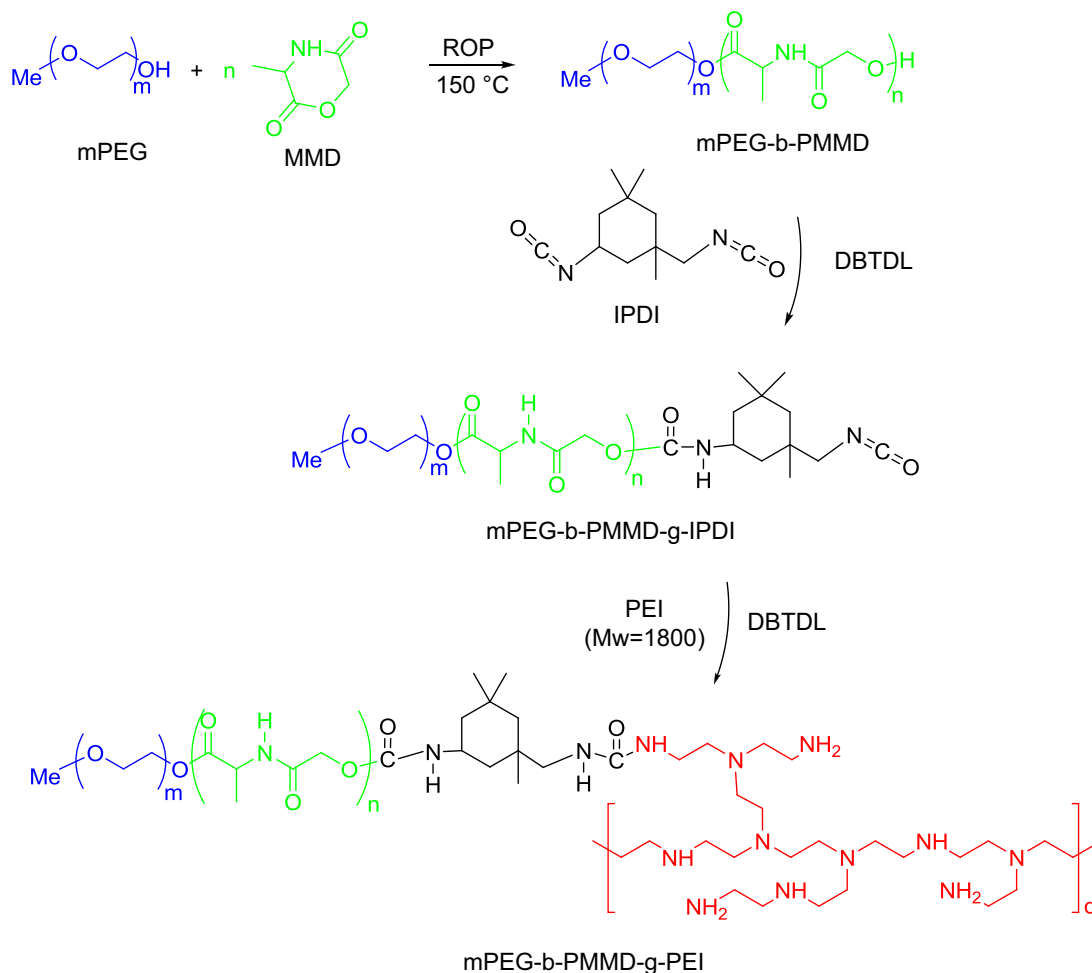
2.6.1. Preparation of MPs

MPs were prepared by using nano-precipitation technology. Briefly, 10.0 mg amphiphilic triblock copolymer (mPEG-b-P(MMD-co-LA)-g-PEI or mPEG-b-P(MMD-co-LA-co-GA)-g-PEI) was dissolved in 1 mL THF. The solution was added dropwise to 10 mL of triple-distilled water stirred at reasonable speed (400–1500 rpm) in a beaker in 1 h. Then the mixture solution was stirred at room temperature for 24 h to remove THF in a fume cupboard; final volume of the solution was adjusted to 10 mL for further experiments.

The mPEG-b-PMMD-g-PEI amphiphilic triblock copolymer only dissolved in DMSO. Therefore, 10.0 mg mPEG-b-PMMD-g-PEI triblock copolymer was dissolved in 1 mL DMSO. The solution was added dropwise to 10 mL of triple-distilled water stirred at suitable speed (400–1500 rpm) in a beaker in 1 h, then the mixture solution was transferred in to a dialysis bag (molecular weight cut off = 3500 Da), the dialysis bag was dipped into the a beaker (1 L) which filled with distilled water, DMSO was removed after 48 h at a low stirring speed (500 rpm), and the distilled water was exchanged every 3 h.

2.6.2. Preparation of MPs/pEGFP-ZNF580 complexes

The plasmid of pEGFP-ZNF580 was diluted to 1 $\mu\text{g}/50 \mu\text{L}$ with PBS buffer (pH = 7.4). The complexes were prepared by adding MPs solution (1 mg/mL) to plasmid solution (containing 1 μg DNA) at various N/P molar ratios (0.5:1, 1:1, 2:1, 4:1, 8:1, 10:1, 20:1). N/P molar ratios were calculated from weight of polymer and plasmid, N content in the polymer and P content in plasmid. Before characterization and further experiments, the complexes were mixed gently and incubated for 30 min at room temperature in a clean bench.



Scheme 1. Synthesis route of mPEG-b-PMMD-g-PEI amphiphilic triblock copolymer. The triblock polymers of mPEG-b-P(MMD-co-LA)-g-PEI and mPEG-b-P(MMD-co-LA-co-GA)-g-PEI were synthesized via the same synthesis route from MMD, LA and/or GA monomer.

Table 1

Molecular weight of amphiphilic triblock copolymers and content of mPEG, MMD, LA, GA and PEI in amphiphilic triblock copolymers, whereas the subscript 1 and 2 stands for samples with different molecule weight.

Sample ID	Content ^a /%					$M_w^b/10^4$	$M_w^c/10^4$	$M_w^c/10^4$	PDI ^c
	mPEG	MMD	LA	GA	PEI				
mPEG-b-PMMD-g-PEI ₁	36	51	0	0	13	1.38	1.34	1.36	1.03
mPEG-b-PMMD-g-PEI ₂	32	57	0	0	11	1.68	1.61	1.64	1.10
mPEG-b-P(MMD-co-LA)-g-PEI ₁	37	15	35	0	13	1.38	1.33	1.32	1.08
mPEG-b-P(MMD-co-LA)-g-PEI ₂	31	11	47	0	11	1.68	1.60	1.61	1.56
mPEG-b-P(MMD-co-LA-co-GA)-g-PEI ₁	38	10	27	11	14	1.38	1.30	1.29	1.43
mPEG-b-P(MMD-co-LA-co-GA)-g-PEI ₂	32	17	28	12	11	1.68	1.58	1.60	1.23

^a Estimated by ¹H NMR.

^b Theoretical molecular weight.

^c Determined by GPC.

2.6.3. Size distribution and zeta potential

The size and zeta potential of MPs and MPs/pEGFP-ZNF580 complexes were measured using a Zetasizer 3000HS (Malvern Instrument, Inc., Worcestershire, UK) at the wavelength of 677 nm with a constant angle of 90°.

2.6.4. Agarose gel electrophoresis

Agarose gel electrophoresis was performed to assess the DNA condensation ability of MPs. The MPs/pEGFP-ZNF580 complexes with various N/P molar ratios ranging from 0.5 to 20 were prepared. The mixture solution was loaded into the agarose gel (0.8%) containing 0.5 µg/mL ethidium bromide. Electrophoresis was performed in 1 × TAE buffer at 100 V for 40 min, UV illuminator was used to indicate the retarded location of the plasmid DNA.

2.6.5. In vitro release

The MPs/pEGFP-ZNF580 complexes at the N/P molar ratio of 10, containing 20 µg pEGFP-ZNF580 in each eppendorf tube, were incubated in 200 µL of Tris–HCl buffer (pH = 7.4) in a shaking incubator at 37 °C. At different time intervals, the complexes solution was centrifuged at 12,000 rpm, –4 °C for 20 min; the supernatant was taken out carefully. Then, the complexes were resuspended with fresh Tris–HCl buffer and reincubated. The adsorption efficiency of plasmid DNA was obtained by measuring the extinction fluorescence with ethidium bromide, the supernatant was analyzed using Cary Eclipse fluorescence spectrometer at excitation wavelength of 524 nm and emission wavelength of 582 nm [24].

2.6.6. Morphology

The morphological study of MPs and MPs/pEGFP-ZNF580 complexes were performed on JME100CXII transmission electron microscope (TEM, JEOL Ltd, Japan). Samples were prepared as the following method [25]. Briefly, MPs solution (1 mg/mL) and various N/P molar ratios (0.5:1, 1:1, 2:1, 4:1, 8:1, 10:1, 20:1) MPs/pEGFP-ZNF580 solutions were dipped onto a carbon-coated copper grid. Then, the carbon-coated copper grid dried in the air for 10 h before taking images.

2.7. Transfection and cytotoxicity

2.7.1. Cell culture

EA.hy926 cells, the human endothelial cell hybridoma line, were purchased from American Type Culture Collection, and were cultured in high glucose DMEM supplemented 10% FBS in 5% CO₂ atmosphere at 37 °C. The next day, the non-adherent cells were discarded, the adherent cells were cultured to 80–90% confluence [13].

2.7.2. In vitro transfection

EA.hy926 cells were seeded in 24-well plate at a density of 1×10^4 cell/well and cultured for 24 h until 80–90% confluence. Before transfection, cells were incubated with serum-free medium for 12 h. MPs/pEGFP-ZNF580 complexes at N/P molar ratio of 10 (1 µg pEGFP-ZNF580 per well) were added into wells. After 4 h, the medium was changed with fresh growth medium (10% FBS DMEM). Then, cells incubated to obtain considerable efficiency of gene transfection, the expression of green fluorescence protein (GFP) in cells was observed under an inverted fluorescent microscope at 12, 24 and 48-h time points.

2.7.3. Protein extraction and western blot analysis

Western blot analysis was performed as reported previously [12]. Briefly, cells were washed twice with 0.1 mol/L PBS (pH = 7.4), and then lysed in RIPA lysis buffer. The concentration of the lysate was determined by a BCA protein assay kit. Cell lysates containing 50 µg of protein were subjected to SDS-PAGE by 15% polyacrylamide resolving gels. Proteins were transferred onto polyvinylidene fluoride membranes and incubated with rabbit anti-human ZNF580 polyclonal antibody after electrophoresis. Proteins were incubated with horseradish peroxidase conjugated to goat anti-rabbit Ig G to assess the protein loading level, and then were incubated with enhanced chemiluminescence reagent and were exposed to film. The belt was analyzed using Image J 2.1. β-Actin antibody was used as a control.

2.7.4. In vitro cytotoxicity

The cytotoxicity of MPs and MPs/pEGFP-ZNF580 complexes was evaluated by MTT assay using PEI ($M_w = 10\,000$) as the control group. Briefly, EA.hy926 cells (1×10^4 cell/well) were seeded in 96-well plate, and cultured for 24 h until 80–90% confluence. Then, the medium was replaced with serum-free medium. After 12 h, the medium was changed with fresh growth medium (10% FBS DMEM). MPs solution and MPs/pEGFP-ZNF580 complexes at various N/P molar ratios were added into the medium. After 48 h, the supernatant was discarded, 20 µL of MTT solution (5 mg/mL) was added to each well and formazan crystals were allowed to form for another 4 h. Then, the medium was removed carefully, 150 µL of DMSO was added to each well, the plate was oscillated in low speed on volatility instrument for 10 min. Optical density (OD) was measured by an ELISA reader (Titertek multiscan MC) at the wavelength of 490 nm. The relative cell viability (%) was calculated using the following formula: (OD490': the absorbance value of experimental wells minus zero wells, avg (OD490C'): the average absorbance value of corrected control wells).

$$\text{Relative cell viability} = \frac{\text{OD490'}}{\text{avg (OD490C')}} \times 100\%$$

2.8. Wound healing assay

The migration capability of EA.hy926 cells transfected by MPs/pEGFP-ZNF580 complexes was assessed using a scratch wound healing assay [26]. Briefly, EA.hy926 cells were transfected with MPs/pEGFP-ZNF580 complexes at the N/P molar ratio of 10; 48 h later, the transfected cells were incubated to produce a nearly confluent cell monolayer in a 6-well plate. A linear wound was subsequently generated in the monolayer using a sterile 200 µL plastic pipette tip. Cellular debris was removed by washing with D-hanks buffer (pH = 7.4). After that, the migration process at different time points (0, 6 and 12 h) was monitored using inverted microscope; the migration area was calculated using Image J 2.1 based on the images after 12 h. The measure of the wounded area was calculated by the following formula: wounded area = length × width, the percentage of migration area was calculated by the following formula: migration area (%) = (wounded area – non-recovered area)/wounded area [27].

2.9. Statistical analysis

All experiments were performed at least three times. Quantitative data are presented as the mean ± S.D. Statistical comparisons were made with Student's *t*-test. *P*-Values (<0.05) were considered to be statistically significant.

3. Results

3.1. Synthesis of amphiphilic triblock copolymers

Triblock amphiphilic copolymers of mPEG-b-PMMD-g-PEI, mPEG-b-P(MMD-co-LA)-g-PEI and mPEG-b-P(MMD-co-LA-co-GA)-g-PEI were synthesized and used as the biodegradable gene carrier materials. As an example, the synthesis route of mPEG-b-PMMD-g-PEI copolymer is shown in Scheme 1. Herein, mPEG was used as the initiator, and expected to form a hydrophilic corona due to its high hydrophilicity and flexibility of the backbone [28]. As an effective cyclopeptide, MMD was copolymerized with LA and/or GA to form the poly(ester amide) structure. Poly(lactide-co-glycolide) (PLGA) copolymers are widely used in clinic as reabsorbable biodegradable material, and in delivery systems for the controlled

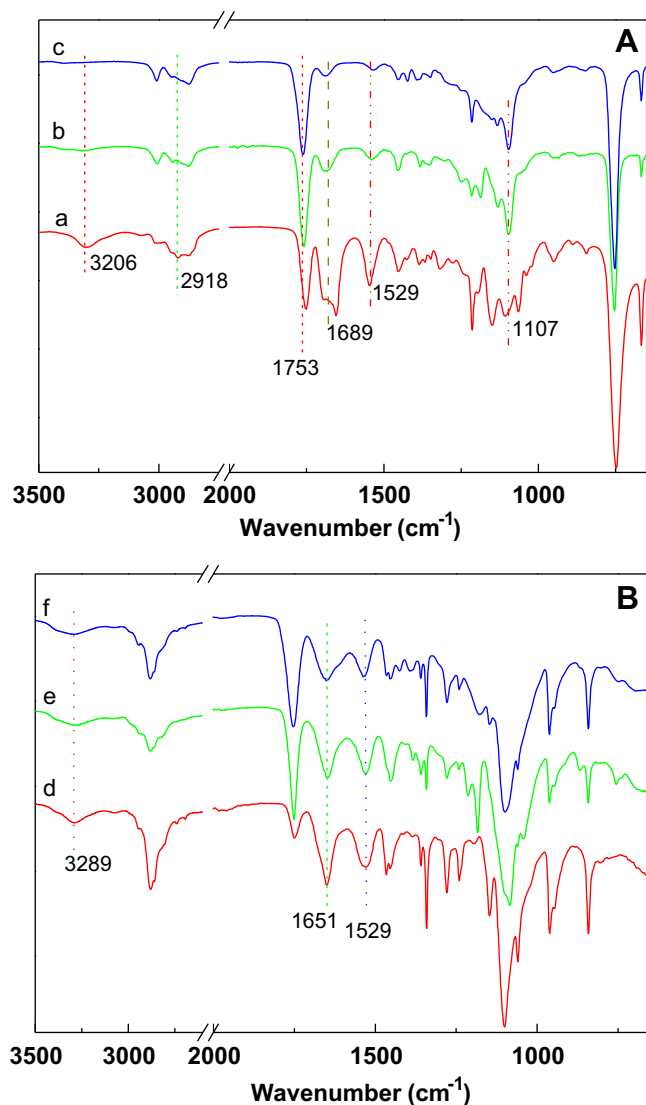


Fig. 1. FT-IR spectra of diblock copolymers (A) and triblock copolymers (B). (a) mPEG-b-PMMD₁ diblock copolymer, (b) mPEG-b-P(MMD-co-LA)₁ diblock copolymer, (c) mPEG-b-P(MMD-co-LA-co-GA)₁ diblock copolymer, (d) mPEG-b-PMMD-g-PEI₁ triblock copolymer, (e) mPEG-b-P(MMD-co-LA)-g-PEI₁ triblock copolymer, (f) mPEG-b-P(MMD-co-LA-co-GA)-g-PEI₁ triblock copolymer.

release of drugs. Furthermore, the triblock polymers of mPEG-b-P(MMD-co-LA)-g-PEI and mPEG-b-P(MMD-co-LA-co-GA)-g-PEI were also synthesized via ROP synthesis route from MMD, LA and/or GA monomer. As shown in Table 1, the molecular weight of triblock copolymers and the content of mPEG, MMD, GA and PEI in copolymers were estimated by ¹H NMR and/or GPC.

As shown in Fig. 1A, diblock copolymers presented a strong signal at 1107 cm⁻¹ which indicated the ether groups of mPEG [29]. The stretching frequency at 1689 cm⁻¹ showed the secondary amide (–NH–) in PMMD segments; the signal at 1753 cm⁻¹ was assigned to the carboxylate group (–O–CO–) in both PMMD and PLGA [30]; the signal at 2918 cm⁻¹ ascribed to methylene group (–CH₂–) in mPEG chain; the broad absorption band at 3206 cm⁻¹ assigned to the stretching of secondary amide (–NH–) group in PMMD [21]. It was found that the characteristic peaks of the secondary amide (–NH–) caused by PMMD was obviously displayed in the diblock copolymers. The FT-IR results suggested that mPEG-b-PMMD₁, mPEG-b-P(MMD-co-LA)₁ and mPEG-b-P(MMD-co-LA-co-GA)₁ diblock copolymers were synthesized successfully.

As shown in Fig. 1B, after the graft of PEI, the symmetric stretching characteristic peaks of primary amine (–NH₂) could be found at 3289 cm⁻¹ and 1651 cm⁻¹, the stretching peaks of secondary amine (–NH–) were observed at 1529 cm⁻¹ [31]. These results indicated that mPEG-b-PMMD-g-PEI₁, mPEG-b-P(MMD-co-LA)-g-PEI₁ and mPEG-b-P(MMD-co-LA-co-GA)-g-PEI₁ triblock copolymers were synthesized perfectly.

The ¹H NMR spectra of diblock copolymer of mPEG-b-PMMD₁ and triblock polymer of mPEG-b-PMMD-g-PEI₁ are illustrated in Fig. 2. The peaks corresponding to mPEG and MMD could be obviously found in the spectrum and assigned as follow, the chemical shift of the protons of diblock copolymer in DMSO-d₆ (Fig. 2A): 1.34 ppm (NH–CH–CH₃, 3H), 3.6–3.8 ppm (O–CH₂–CH₂, 4H), 4.3–4.4 ppm (NH–CH–CH₃, 1H) [21], 4.5–4.8 ppm (CO–CH₂–O, 2H), and 8.3–8.5 ppm (CH–NH, 1H). ¹H NMR spectrum of triblock copolymer (Fig. 2B) showed two characteristic resonances of protons at δ 2.4 ppm – 3.2 ppm (–NH–CH₂–CH₂–, PEI segment), and at 0.8 ppm – 0.9 ppm (–CH₃, IPDI residue). These results suggested that mPEG-b-PMMD₁ and mPEG-b-PMMD-g-PEI₁ copolymers were synthesized successfully.

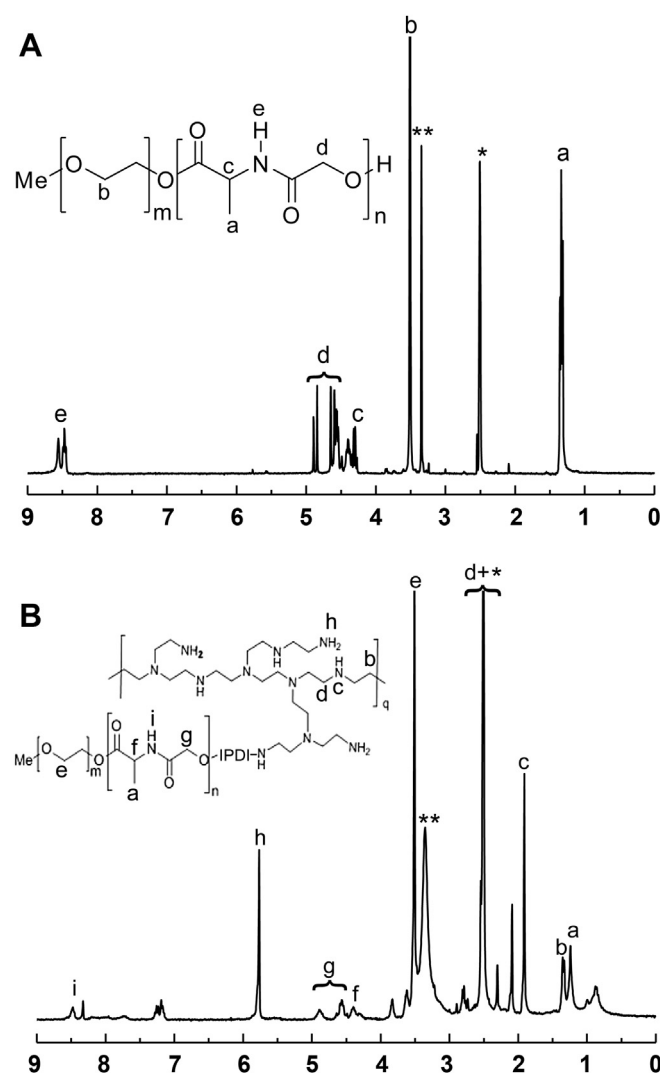


Fig. 2. ¹H NMR spectra of mPEG-b-PMMD₁ diblock copolymer and mPEG-b-PMMD-g-PEI₁ amphiphilic triblock copolymer in DMSO-d₆ solvent. (A) ¹H NMR spectrum of mPEG-b-PMMD₁ diblock copolymer, (B) ¹H NMR spectrum of mPEG-b-PMMD-g-PEI₁ amphiphilic triblock copolymer, * = DMSO peaks; ** = H₂O peaks.

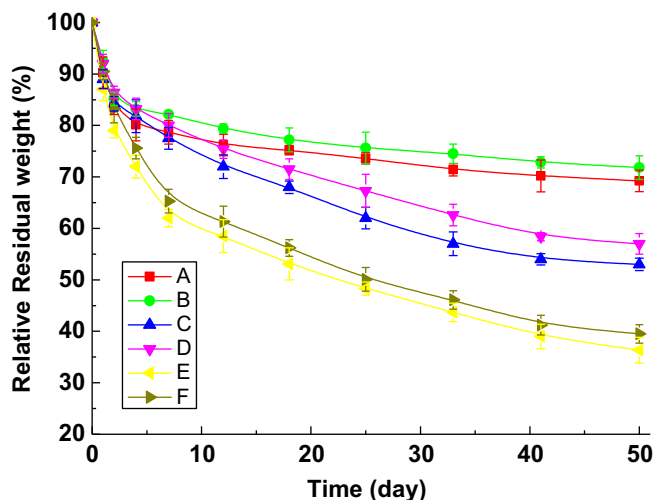


Fig. 3. Residual weight of the copolymers in PBS (pH = 7.4), at 37 °C under constant shaking at 30 rpm. (A) mPEG-b-PMMD-g-PEI₁ triblock copolymer, (B) mPEG-b-PMMD-g-PEI₂ triblock copolymer, (C) mPEG-b-P(MMD-co-LA)-g-PEI₁ triblock copolymer, (D) mPEG-b-P(MMD-co-LA)-g-PEI₂ triblock copolymer, (E) mPEG-b-P(MMD-co-LA-co-GA)-g-PEI₁ triblock copolymer, (F) mPEG-b-P(MMD-co-LA-co-GA)-g-PEI₂ triblock copolymer. Error bars represent the standard deviations ($n = 3$).

3.2. Characterization of copolymers

3.2.1. Degradation behavior of the amphiphilic triblock copolymers

The degradation behavior of the amphiphilic triblock copolymers was tested *in vitro* in PBS (pH = 7.4), at 37 °C under constant shaking at 30 rpm. After 50 days, the relative residual weight of mPEG-b-PMMD-g-PEI copolymers decreased to 69.3% and 71.8%. mPEG-b-P(MMD-co-LA)-g-PEI copolymers degraded faster than mPEG-b-PMMD-g-PEI copolymers, and their relative residual weight was found to be 53.0% and 57.0%. Furthermore, mPEG-b-P(MMD-co-LA-co-GA)-g-PEI copolymers showed the fastest weight loss, and the relative residual weight was only 36.3% and 39.5%.

Crystallinity and hydrophilicity are main factors which effect the degradation of polydepsipeptides based copolymers or homopolymers [32]. The homopolymers, for example, PLLA and PMMD, usually have a relative high degree of crystallinity, which results in low degradation rate. In random copolymers of L-LA or GA and MMD, the polymer chains consist of random amide groups and ester groups, as well as $-\text{CH}_3$ side groups. This ununiform structures hinder the crystallinity of the random copolymers.

Fig. 3 showed that the degradation process of the amphiphilic triblock copolymers had two stages. During the first stage, the residual weight of all copolymers decreased quickly within the initial 4 days, which is due to the hydrolysis of the ester bonds in the hydrophobic segments (PMMD, P(MMD-co-LA) and P(MMD-co-LA-

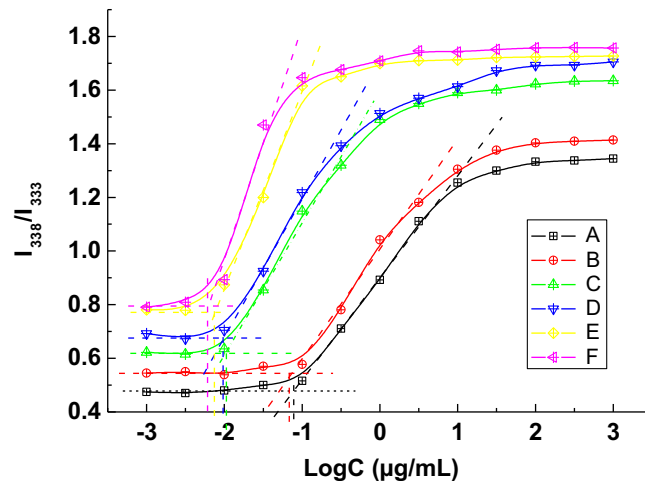


Fig. 4. Fluorescence intensity ratio variation of I_{338}/I_{333} for pyrene emission against the concentration of copolymers. (A) mPEG-b-PMMD-g-PEI₁ triblock copolymer, (B) mPEG-b-PMMD-g-PEI₂ triblock copolymer, (C) mPEG-b-P(MMD-co-LA)-g-PEI₁ triblock copolymer, (D) mPEG-b-P(MMD-co-LA)-g-PEI₂ triblock copolymer, (E) mPEG-b-P(MMD-co-LA-co-GA)-g-PEI₁ triblock copolymer, (F) mPEG-b-P(MMD-co-LA-co-GA)-g-PEI₂ triblock copolymer.

co-GA)) nearly connected with hydrophilic chains (PEG and PEI). In this stage, PEG and PEI were dissolved along with the degradation of the ester bonds in PBS. During the second stage, the crystallinity and hydrophilicity of the copolymers became the major factors which affected the diffusion of water and degradation of ester group, because most of the hydrophilic chains had been dissolved. In this stage, the mPEG-PMMD-g-PEI copolymers degraded slowly because of the high degree crystallinity of PMMD segments. But when MMD was copolymerized with LA and/or GA, the crystallinity of P(MMD-co-LA) and P(MMD-co-LA-co-GA) copolymer segments decreased greatly. This low crystallinity was favor for the degradation of these copolymers.

3.2.2. CMC of triblock copolymers

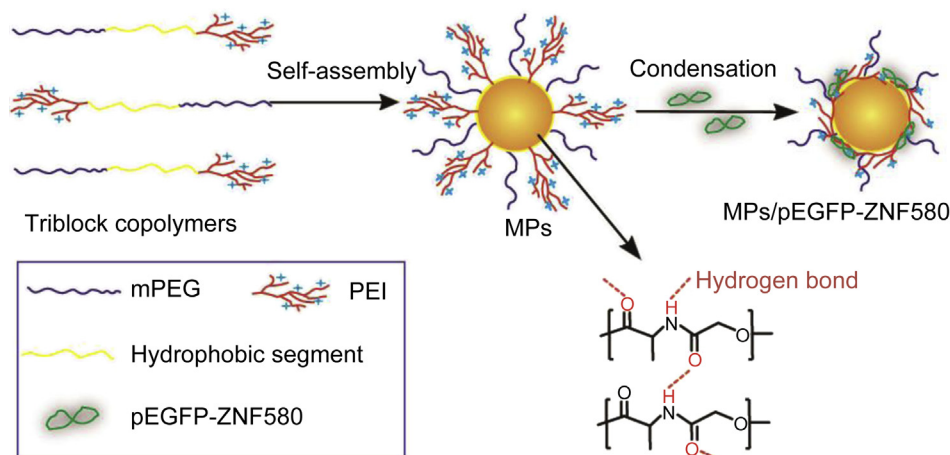
The CMC values of the triblock copolymers were determined by fluorescent determination method and listed in Table 2. Compared with the poly(depsipeptide-co-PDO)-PEG-poly(depsipeptide-co-PDO) triblock copolymers reported by our research group previously [33], these triblock copolymers showed low CMC values. This might be attributed to the higher hydrophobicity of the cores which were formed from PMMD, P(MMD-co-LA) and P(MMD-co-LA-co-GA) segments of the block copolymers. As expected, the hydrophobic polydepsipeptide could easily form a core. The strong hydrogen-bond interaction in polydepsipeptides as well as between polydepsipeptides and LA/GA reduces the fluidity of core and enhances the stability of micelle structure [34], and it might also lead to low CMC values (Fig. 4).

Table 2
Size, zeta potential and CMC value of MPs.

Sample ID	Size (nm)	PDI ^a	Z. P. ^a (mV)	CMC ^b (μg/mL)
mPEG-b-PMMD-g-PEI ₁	203 ± 11.9	0.31 ± 0.01	32.0 ± 0.7	0.079
mPEG-b-PMMD-g-PEI ₂	200.6 ± 9.6	0.34 ± 0.09	34.8 ± 0.9	0.051
mPEG-b-P(MMD-co-LA)-g-PEI ₁	189.1 ± 11.5	0.26 ± 0.02	26.5 ± 1.0	0.013
mPEG-b-P(MMD-co-LA)-g-PEI ₂	186.1 ± 7.8	0.36 ± 0.06	25.8 ± 0.8	0.009
mPEG-b-P(MMD-co-LA-co-GA)-g-PEI ₁	153.6 ± 9.6	0.28 ± 0.01	20.0 ± 0.6	0.006
mPEG-b-P(MMD-co-LA-co-GA)-g-PEI ₂	151.2 ± 10.6	0.22 ± 0.03	22.0 ± 0.4	0.003

^a PDI: Polydispersity index; Z. P: Zeta potential (Temperature = 25 °C, pH = 7.4).

^b CMC: Critical micelle concentration, determined in deionized water.



Scheme 2. MPs were prepared by the self-assembly of amphiphilic triblock copolymers, and MPs/pEGFP-ZNF580 complexes by condensation with pEGFP-ZNF580. The self-assembly process was illustrated by the example of mPEG-b-PMMD-g-PEI₁ triblock copolymer, the PMMD hydrophobic segments act as the core, PEI and mPEG form the cationic shell and hydrophilic corona. P(MMD-co-LA) or poly(MMD-co-LA-co-GA) segments act as the hydrophobic core for other MPs.

3.2.3. Morphology study of MPs and MPs/pEGFP-ZNF580 complexes

Amphiphilic triblock copolymers can assemble into core-shell structure MPs in aqueous solution, namely, PMMD, P(MMD-co-LA) or P(MMD-co-LA-co-GA) of the triblock copolymers act as hydrophobic segments to form the core of MPs, while PEI and mPEG form the cationic shell and hydrophilic corona. As shown in Scheme 2, the self-assembly process was illustrated using mPEG-b-PMMD₁ as an example. Herein, mPEG is used as a water barrier that prevents proteins from approaching the surface. PEG should also reduce the tendency of particles to aggregate by steric stabilization [35]. Low molecular weight PEI is usually suggested to be used for gene delivery because of its low cytotoxicity compared with high molecular weight PEI, but it almost had no transfection efficacy [17]. In order to overcome this obstacle, in the present study, we prepared the MPs by self-assembly, every MPs was formed from many triblock copolymer chains, the hydrophobic core of the MPs acted as a crosslinking point which linked numbers of PEI and PEG chains, thus the PEI and PEG chains on the surface of MPs can endow them with high hydrophilic and high positive charge characteristic.

The hydrodynamic diameter and zeta potential of MPs were measured by nanoparticle size and zeta potential analyzer. The mean size and zeta potential value are summarized in Table 2, the size of MPs ranged from 151 to 203 nm with a reasonable polydispersity index (PDI < 0.4); the zeta potential ranged from 20.0 to 34.8 mV. As shown in Scheme 2, the hydrogen bond caused by

polydepsipeptide in the hydrophobic segments was an important factor to account for the size of MPs. The strong hydrogen bonding effect increases the stability of the hydrophobic core, thus results in the formation of larger particles [21]. In the following study, mPEG-b-PMMD-g-PEI₁, mPEG-b-P(MMD-co-LA)-g-PEI₁ and mPEG-b-P(MMD-co-LA-co-GA)-g-PEI₂ based MPs were used due to their different size and positive potential.

MPs/pEGFP-ZNF580 complexes were prepared by mixing the MPs solution with pEGFP-ZNF580 in PBS (pH = 7.4) at room temperature and allowed for 30 min to form complexes. The TEM images of mPEG-b-PMMD-g-PEI₁ based MPs and its complexes were shown in Fig. 5. The morphology of MPs and MPs/pEGFP-ZNF580 complexes (N/P = 10) exhibited spherical structure. However, the MP sizes (about 160 nm) measured by TEM were smaller than those obtained by nanoparticle size and zeta potential analyzer. The particle sizes measured by nanoparticle size and zeta potential analyzer were obtained in hydrated state in solution, while those obtained by TEM had been dried after being dropped onto carbon-coated copper meshes.

The formation of MPs/pEGFP-ZNF580 complexes with appropriate size (100–200 nm) and positive charged surface (10–30 mV) is an important prerequisite for polycations which are used as gene carriers [36,37]. The size and zeta potential of MPs/pEGFP-ZNF580 complexes were measured at different N/P molar ratios. When the N/P molar ratio rose from 5 to 20, the diameter of mPEG-b-P(MMD-

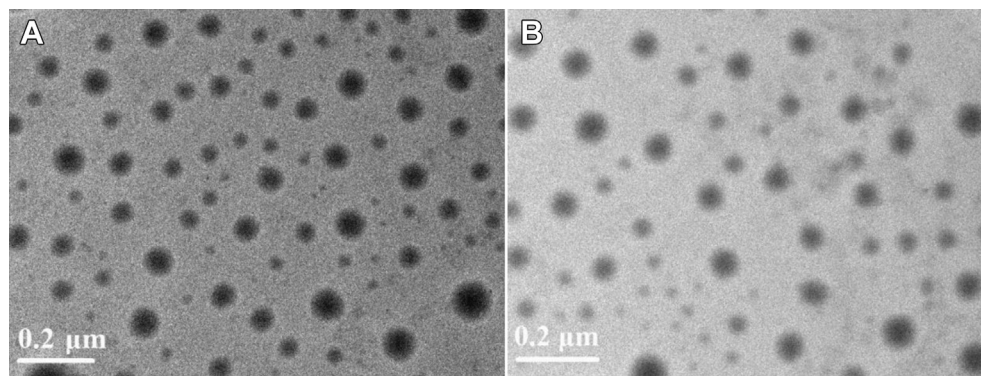


Fig. 5. TEM images of MPs and MPs/pEGFP-ZNF580 complexes. (A) MPs formed by mPEG-b-PMMD-g-PEI₁ triblock copolymer, (B) mPEG-b-PMMD-g-PEI₁ based MPs/pEGFP-ZNF580 complexes prepared from mPEG-b-PMMD-g-PEI₁ based MPs and pEGFP-ZNF580.

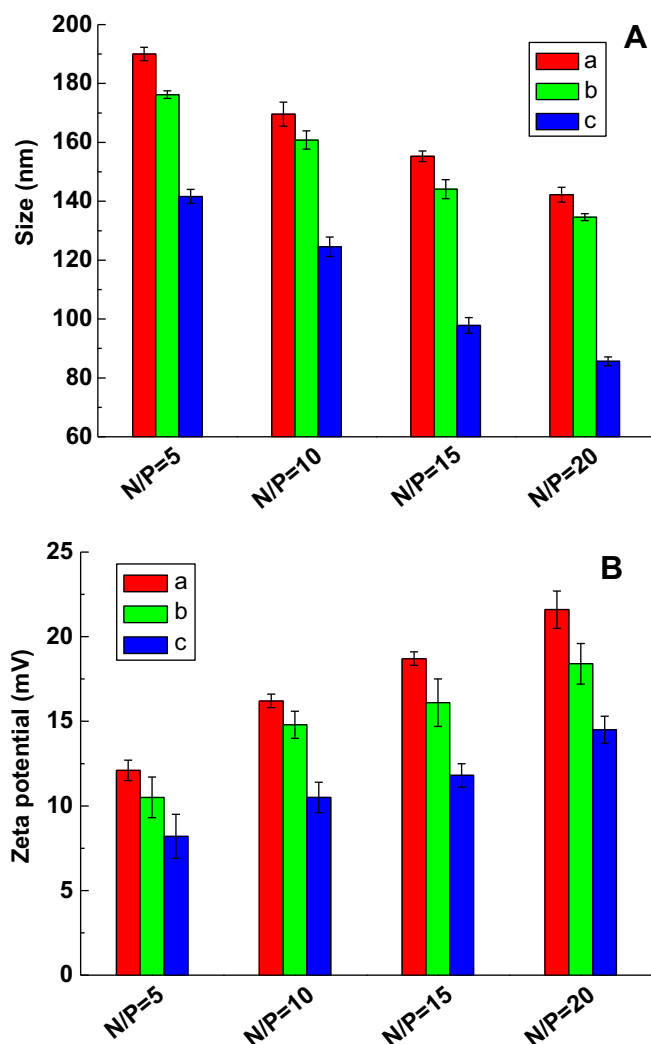


Fig. 6. Microparticle size (A) and zeta potential (B) of MPs/pEGFP-ZNF580 complexes at different N/P ratios. (a) mPEG-b-PMMD-g-PEI₁ based MPs/pEGFP-ZNF580 complexes, (b) mPEG-b-P(MMD-co-LA)-g-PEI₁ based MPs/pEGFP-ZNF580 complexes, (c) mPEG-b-P(MMD-co-LA-co-GA)-g-PEI₁ based MPs/pEGFP-ZNF580 complexes.

co-LA-co-GA)-g-PEI₁ based MPs/pEGFP-ZNF580 complexes changed from 86 to 140 nm (Fig. 6A), this results indicated that after the condensation with pEGFP-ZNF580, the size of MPs/pEGFP-ZNF580 complexes became slightly smaller than the MPs (189.1 nm). The declining trend of the complex sizes is mainly due to the high N/P molar ratio that made the complexes evolved into more compact entities where DNA molecules are highly compressed [38]. It is noteworthy that at N/P of 10, the average

hydrodynamic diameters of the mPEG-b-PMMD-g-PEI₁, mPEG-b-P(MMD-co-LA)-g-PEI₁ and mPEG-b-P(MMD-co-LA-co-GA)-g-PEI₁ based MPs/pEGFP-ZNF580 complexes were 169.6, 160.8 and 124.5 nm, which is suitable to be applied for endocytic cellular uptake [39].

The zeta potential of the complex at different N/P molar ratios presented net positive charges as shown in Fig. 6B. With the increase of N/P molar ratio, the net positive charges of the complexes were increased. Suitable net positive charges on the surface of MPs provide a guarantee for high transfection, because the initial electrostatic interactions between positively charged MPs/pEGFP-ZNF580 complexes and negatively charged cell membrane play an important role in the endocytosis.

3.2.4. Agarose gel electrophoresis

Effective condensation of negatively charged pEGFP-ZNF580 into MPs through electrostatic interactions is of great importance for well-designed gene carriers. Therefore, a gel retardation assay was employed to verify the successful binding between MPs and pEGFP-ZNF580. Before gel retardation assay, MPs/pEGFP-ZNF580 complexes with different N/P molar ratios were incubated at room temperature for 30 min. The images of gel retardation assay were obtained as shown in Fig. 7, at the N/P molar ratio of 8, the plasmids of pEGFP-ZNF580 were bound totally by mPEG-b-PMMD-g-PEI₁ based MPs; when the N/P rose to 10, the plasmids of pEGFP-ZNF580 could be bound completely by mPEG-b-P(MMD-co-LA)-g-PEI₁ and mPEG-b-P(MMD-co-LA-co-GA)-g-PEI₁ based MPs. Results showed that these MPs exhibited different binding ability, the main reason account for this phenomenon is that the zeta potential of the mPEG-b-PMMD-g-PEI₁ based MPs is the highest among these MPs (Table 2), high positive potential endow these MPs with the strong binding ability to the plasmids.

As we know, MPs with or without pEGFP-ZNF580 are too large to diffuse through the agarose matrix, therefore, only pEGFP-ZNF580, which was not bound in the shell of MPs is able to migrate to the positive electrode in the same manner as the naked pEGFP-ZNF580 [40]. In the following study, the N/P ratio of 10 was selected due to the perfectly binding effect.

3.2.5. In vitro release

It is an important property for gene carriers in gene therapy to obtain an ideal sequential release of gene [10]. In order to investigate the gene release from MPs/pEGFP-ZNF580 complexes, the *in vitro* release assay was carried out. As shown in Fig. 8, during the first week, an initial increase in release was observed for the complexes. After 25 days, about 90.3% of plasmids were released from mPEG-b-P(MMD-co-LA-co-GA)-g-PEI₁ based MPs/pEGFP-ZNF580 complexes, about 84% and 72.4% of the pEGFP-ZNF580 plasmids were released from the mPEG-b-P(MMD-co-LA)-g-PEI₁ and mPEG-b-PMMD-g-PEI₁ based MPs/pEGFP-ZNF580 complexes.

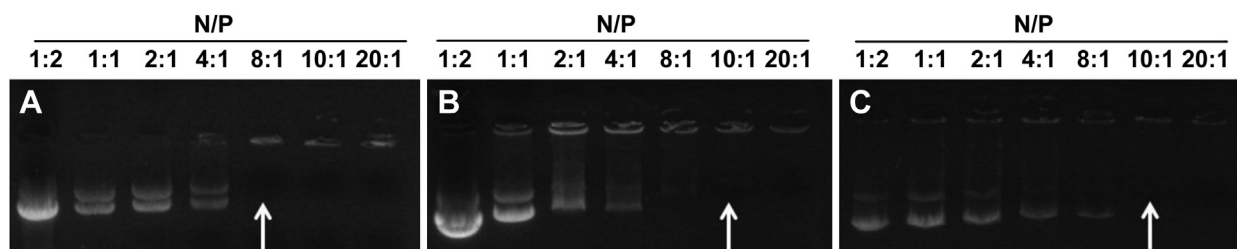


Fig. 7. Agarose gel electrophoresis of MPs/pEGFP-ZNF580 complexes at various N/P molar ratios. (A) mPEG-b-PMMD-g-PEI₁ based MPs/pEGFP-ZNF580 complexes at different N/P molar ratios, (B) mPEG-b-P(MMD-co-LA)-g-PEI₁ based MPs/pEGFP-ZNF580 complexes at different N/P molar ratios, and (C) mPEG-b-P(MMD-co-LA-co-GA)-g-PEI₁ based MPs/pEGFP-ZNF580 complexes at different N/P molar ratios. The arrows indicate the N/P ratios where the DNA mobility is completely retarded.

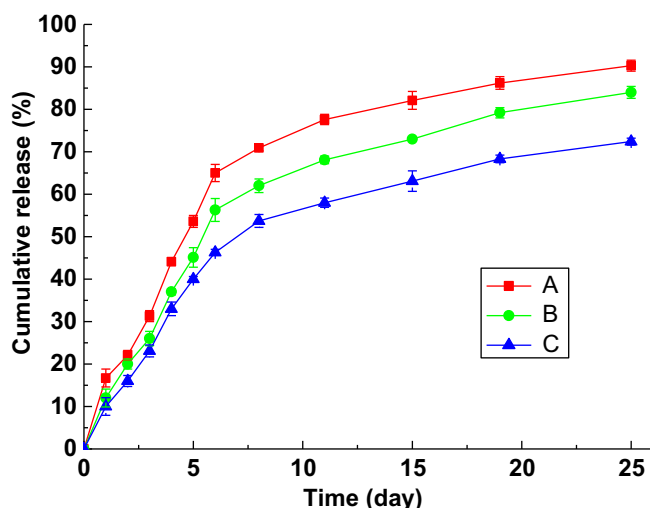


Fig. 8. Cumulative release of pEGFP-ZNF580 from different MPs/pEGFP-ZNF580 complexes at the N/P molar ratio of 10 in Tris–HCl buffer at 37 °C (pH = 7.4). (A) Cumulative release form mPEG-b-P(MMD-co-LA-co-GA)-g-PEI₁ based MPs/pEGFP-ZNF580 complexes, (B) Cumulative release form mPEG-b-P(MMD-co-LA)-g-PEI₁ based MPs/pEGFP-ZNF580 complexes, (C) Cumulative release form mPEG-b-PMMD-g-PEI₁ based MPs/pEGFP-ZNF580 complexes.

During the initial 6 days, all of the complexes showed a rapid nucleic acid release behavior. After 25 days, the cumulative release of pEGFP-ZNF580 from the mPEG-b-P(MMD-co-LA-co-GA)-g-PEI₁ based complexes was the highest among these complexes. This phenomenon can be explained by the flowing analysis, at the initial 6 days, some hydrophilic chains (PEI or PEG) might be hydrolyzed and dissolve out quickly, therefore, many plasmids were also released with them. After 25 days, the cumulative release of plasmids from mPEG-b-P(MMD-co-LA-co-GA)-g-PEI₁ based MPs was the highest than others, the main reason is that degradation of them was more faster than others as shown in Fig. 3. The results

indicated that with the explored MPs/pEGFP-ZNF580 complexes, the release of plasmid could be maintained at least for 25 days.

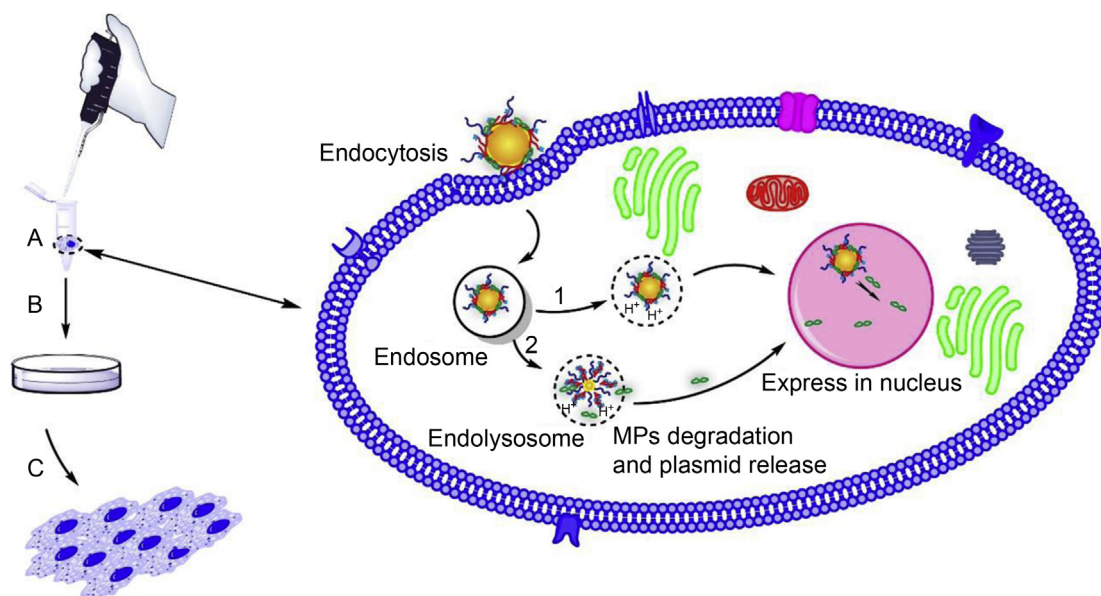
3.3. Transfection and cytotoxicity

3.3.1. In vitro transfection

When MPs/pEGFP-ZNF580 complexes are cultured with EA.hy926 cells in the medium, the complexes can be transported into cells by endocytosis, after escape from endolysosome, the complexes or pEGFP-ZNF580 enter into the nucleus through path 1 or 2, finally, pEGFP-ZNF580 effectively express in the nucleus. By this way, the proliferation of EA.hy926 cells could be promoted greatly (Scheme 3).

In order to determine qualitatively whether the pEGFP-ZNF580 has been transfected into the EA.hy926 cells, the expression of green fluorescence protein (GFP) in ECs was observed under an inverted fluorescent microscope at 12, 24 and 48-h time points. ECs were transfected with mPEG-b-PMMD-g-PEI₁, mPEG-b-P(MMD-co-LA)-g-PEI₁ and mPEG-b-P(MMD-co-LA-co-GA)-g-PEI₁ based MPs/pEGFP-ZNF580 complexes at the N/P molar ratio of 10 using the same concentration (30 µg pEGFP-ZNF580 complexes per volume medium (mL)). Cells treated with Lipofectamine™ 2000 were used as the positive control, and cells without treatment as the negative control. Green fluorescence images of the EA.hy926 cells at different time points were taken by an inverted fluorescence microscope. After 48 h a large proportion of cells with green fluorescent could be observed by the inverted fluorescence microscope (Fig. 9), which indicated that the plasmids had been transfected and expressed successfully in EA.hy926 cells.

Western bolt detection was used to quantitatively characterize the expression of ZNF580 gene in cells. We selected normal cells as negative control, cells transfected by MPs/pEGFP-ZNF580 complexes as test groups, and cells transfected by Lipofectamine™ 2000 as positive control. As shown in Fig. 10, after 48 h of transfection, the relative protein level of cells treated with the mPEG-b-PMMD-g-PEI₁ based MPs/pEGFP-ZNF580 complexes reached to 35.74%, furthermore, that of cells treated with mPEG-b-P(MMD-co-LA)-g-



Scheme 3. The process of transfection and proliferation promoted by biodegradable MPs/pEGFP-ZNF580 complexes. (A) The MPs/pEGFP-ZNF580 complexes at the N/P ratio of 10 were mixed with ECs in the serum-free medium, then the MPs/pEGFP-ZNF580 complexes was transfected into ECs via endocytosis, through path 1 or 2 plasmids of pEGFP-ZNF580 enter into nucleus, (B) After 4 h, the ECs were cultured with fresh growth medium (10% FBS DMEM), (C) By rapid endothelialization, a living functional layer of ECs was formed.

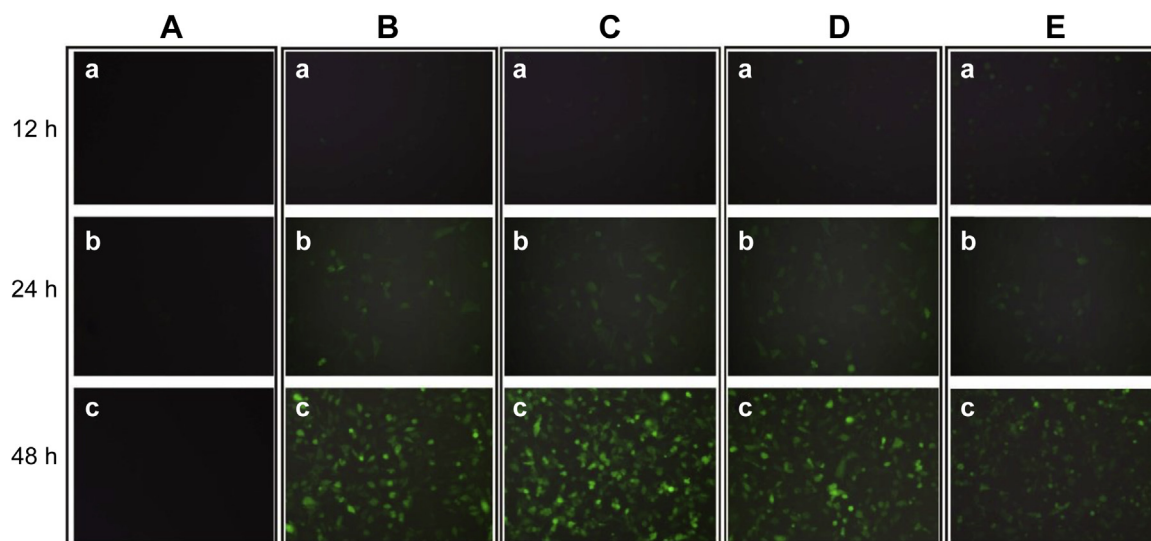


Fig. 9. Fluorescence images of EA.hy926 cells transfected by MPs/pEGFP-ZNF580 complexes at the N/P molar ratio of 10 and time intervals. (A) Cells without treated with MPs/pEGFP-ZNF580 complexes and Lipofectamine™ 2000 served as the negative control group, (B) Cells treated with the mPEG-b-PMMD-g-PEI₁ based MPs/pEGFP-ZNF580 complexes, (C) Cells treated with the mPEG-b-P(MMD-co-LA)-g-PEI₁ based MPs/pEGFP-ZNF580 complexes, (D) Cells treated with the mPEG-b-P(MMD-co-LA-co-GA)-g-PEI₁ based MPs/pEGFP-ZNF580 complexes, (E) Lipofectamine™ 2000 group is the positive control group.

PEI₁ and mPEG-b-P(MMD-co-LA-co-GA)-g-PEI₁ based MPs/pEGFP-ZNF580 complexes reached to 45.61% and 46.11%, respectively. The rapid degradation of mPEG-b-P(MMD-co-LA-co-GA)-g-PEI₁ tri-block copolymer (Fig. 3) provided a fast release of pEGFP-ZNF580 (Fig. 8). This might be the reason for the highest relative protein level exhibited by mPEG-b-P(MMD-co-LA-co-GA)-g-PEI₁ based complexes. These results indicated that pEGFP-ZNF580 was expressed successfully when they released from the MPs/pEGFP-ZNF580 complexes.

3.3.2. In vitro cytotoxicity

The cytotoxicity associated with PEI based nanoparticles has been a concern as gene carrier. Herein, the toxicity of mPEG-b-PMMD-g-PEI₁, mPEG-b-P(MMD-co-LA)-g-PEI₁ and mPEG-b-P(MMD-co-LA-co-GA)-g-PEI₁ based MPs and their MPs/pEGFP-ZNF580 complexes were evaluated by MTT assay using PEI (Mw = 10000) as a control group. As shown in Fig. 11, the relative cell viability of MPs and their MPs/pEGFP-ZNF580 complexes was much higher than PEI at the same concentration; the relative cell

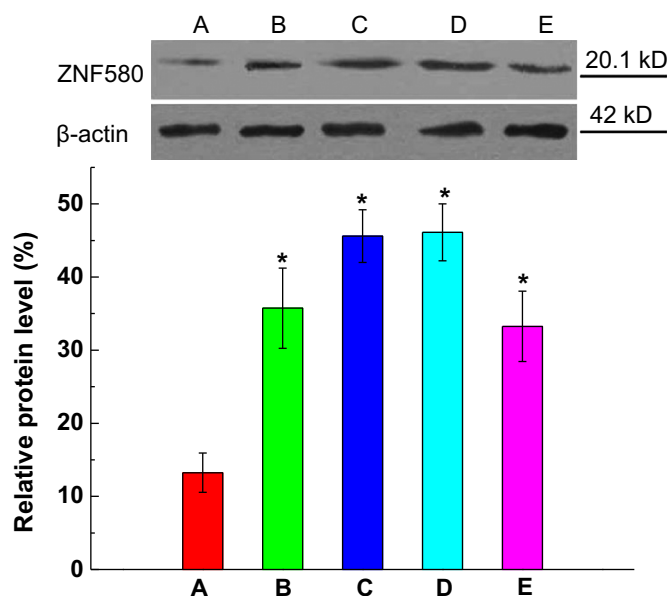


Fig. 10. Western blot analysis for ZNF580 protein expression in EA.hy926 cells transfected by different complexes and Lipofectamine™ 2000 after 48 h. (A) Cells without treated with MPs/pEGFP-ZNF580 complexes and Lipofectamine™ 2000 served as the negative control group, (B) Cells treated with the mPEG-b-PMMD-g-PEI₁ based MPs/pEGFP-ZNF580 complexes, (C) Cells treated with the mPEG-b-P(MMD-co-LA)-g-PEI₁ based MPs/pEGFP-ZNF580 complexes, (D) Cells treated with the mPEG-b-P(MMD-co-LA-co-GA)-g-PEI₁ based MPs/pEGFP-ZNF580 complexes, (E) Lipofectamine™ 2000 group is the positive control group. (\bar{x} + SD, $n = 3$, * $p < 0.05$ vs. A group).

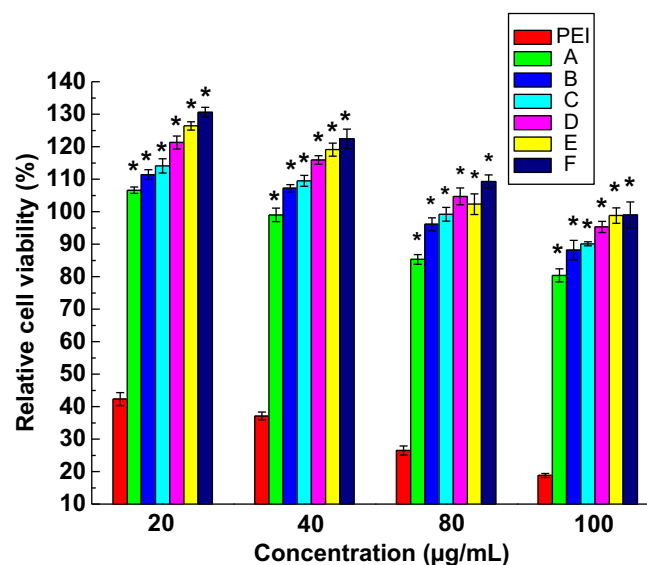


Fig. 11. Relative cell viability of EA.hy926 cells after 48 h of treatment with different concentration MPs and MPs/pEGFP-ZNF580 complexes at N/P molar ratio of 10. Cells treated with PEI (Mw = 10000) served as the control group, (A) Cells treated with the mPEG-b-PMMD-g-PEI₁ based MPs, (B) Cells treated with the mPEG-b-P(MMD-co-LA)-g-PEI₁ based MPs, (C) Cells treated with the mPEG-b-P(MMD-co-LA-co-GA)-g-PEI₁ based MPs, (D) Cells treated with the mPEG-b-PMMD-g-PEI₁ based MPs/pEGFP-ZNF580 complexes, (E) Cells treated with the mPEG-b-P(MMD-co-LA)-g-PEI₁ based MPs/pEGFP-ZNF580 complexes, (F) Cells treated with the mPEG-b-P(MMD-co-LA-co-GA)-g-PEI₁ based MPs/pEGFP-ZNF580 complexes, (\bar{x} + SD, $n = 6$, * $p < 0.05$ vs. PEI group).

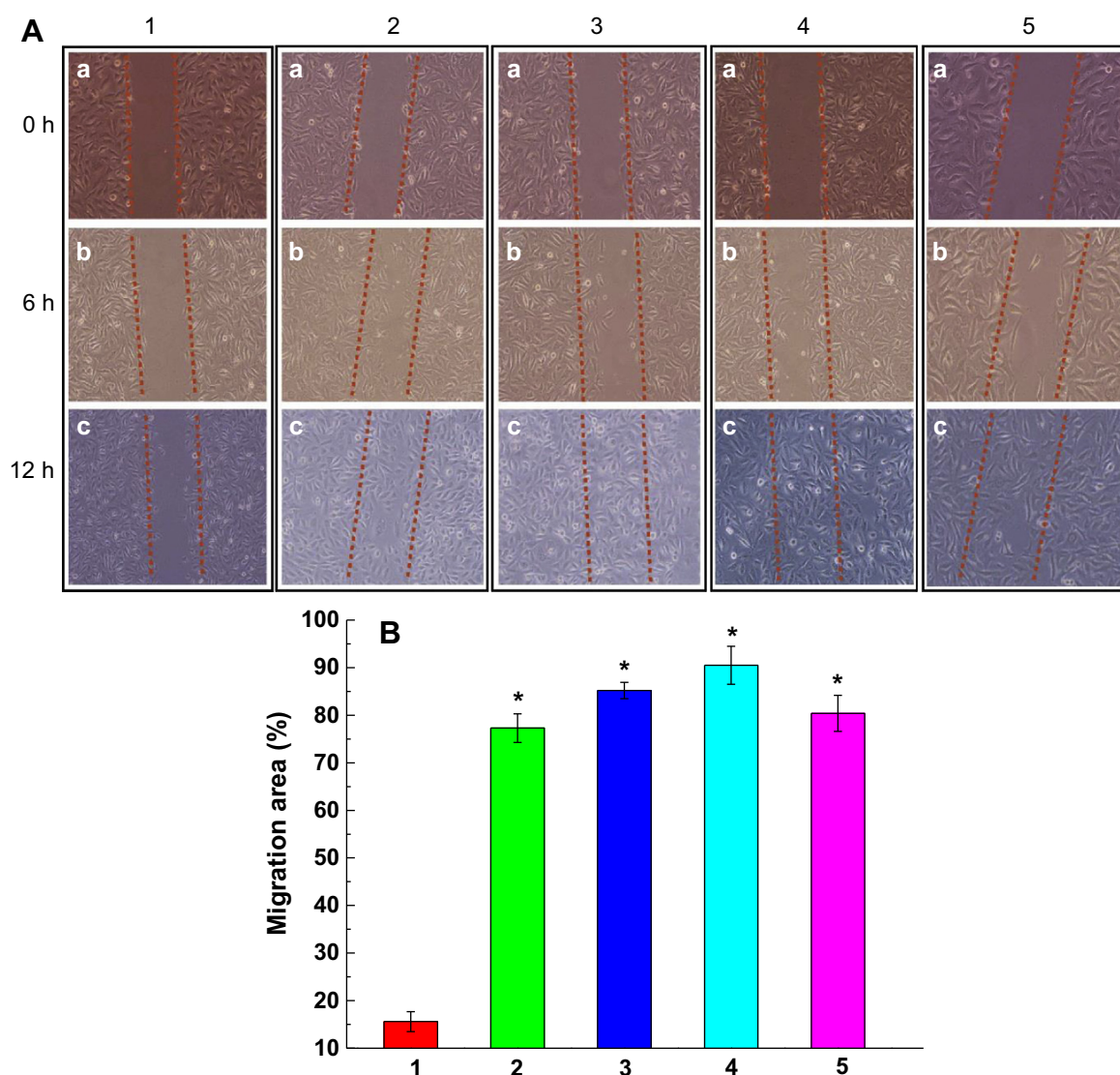


Fig. 12. Migration process of EA.hy926 cells at different time points (A) and migration area (B) after 12 h calculated by Image-Pro Plus (6.0). (1) Cells without treated with MPs/pEGFP-ZNF580 complexes served as the negative control group, (2) Cells treated with the mPEG-b-PMMD-g-PEI₁ based MPs/pEGFP-ZNF580 complexes, (3) Cells treated with the mPEG-b-P(MMD-co-LA)-g-PEI₁ based MPs/pEGFP-ZNF580 complexes, (4) Cells treated with the mPEG-b-P(MMD-co-LA-co-GA)-g-PEI₁ based MPs/pEGFP-ZNF580 complexes, (5) Cells treated with Lipofectamine™ 2000 as the positive control group. ($\bar{x} \pm SD$, $n = 3$, * $p < 0.05$ vs. control group).

viability of their MPs/pEGFP-ZNF580 complexes was relatively higher than that of their MPs at the same concentration.

MPs/pEGFP-ZNF580 complexes only showed mild cytotoxicity (cell viability >80%) even at the high concentration (80 $\mu\text{g/mL}$). This phenomenon can be explained by the neutralization between positive and negative charges [41]. When plasmids of pEGFP-ZNF580 were adsorbed to the surface of MPs, the positive charges of PEI were partly neutralized by the negative charges of them, which minimize the direct contact of the positive charge with the cell membrane, this is the main reason for the low toxicity of MPs/pEGFP-ZNF580 complexes [42].

Low cytotoxicity also is one of the prerequisite for *in vivo* application of polymeric gene carrier. We excitedly demonstrated that the MPs and their MPs/pEGFP-ZNF580 complexes at low concentration (20 $\mu\text{g/mL}$) not only exhibited non-cytotoxicity, but also promoted the cells proliferation. The main reason is that the introduction of PEG chains which formed a hydration layer on the surface of MPs and at the same time the degradation product (L-alanine) released from the hydrophobic core might stimulate the

proliferation of ECs via a signal pathway [43]. These results manifested that these biodegradable MPs should be a suitable gene carrier with non-cytotoxicity.

3.4. Cell migration

Cells migration and proliferation play a vital role in the wound healing process, the scratch assay has been used to study the proliferation/migration properties of different cell lines [26], and is an experimentally well-developed and easy protocol for analyzing cell migration *in vitro*. EA.hy926 cells were transfected with MPs/pEGFP-ZNF580 complexes at the N/P molar ratio of 10. After 48 h, a monolayer of EA.hy926 cells was formed in a 6-well plate *in vitro*. An artificial scratch with parallel borders was mechanically created as shown in Fig. 12A(a). Subsequently, the cells migrated to close this “wound” scratch, the time course of the migration process at different time intervals was monitored by capturing images, and the migration area was calculated by Image-Pro Plus (6.0).

Our study demonstrated a significant effect of MPs/pEGFP-ZNF580 complexes on the proliferation and migration of ECs. As shown in Fig. 12(B), since the form of scratch, after 12 h, the migration area of cells transfected by mPEG-b-P(MMD-co-LA-co-GA)-g-PEI₁ based MPs/pEGFP-ZNF580 complexes increased to $90.5 \pm 4.0\%$, while that of cells transfected by mPEG-b-PMMD-g-PEI₁ and mPEG-b-P(MMD-co-LA)-g-PEI₁ based MPs/pEGFP-ZNF580 complexes only increased to $77.3 \pm 3.0\%$ and $85.2 \pm 1.7\%$, respectively. It was obviously found that mPEG-b-P(MMD-co-LA)-g-PEI₁ and mPEG-b-P(MMD-co-LA-co-GA)-g-PEI₁ based MPs/pEGFP-ZNF580 complexes showed high migration and proliferation effect compared with the positive group ($80.4 \pm 3.8\%$). These results suggested that after transfection, 60 h later, the rapid endothelialization was promoted greatly by the expression of ZNF580 genes released from these MPs/pEGFP-ZNF580 complexes.

4. Discussion

Rapid endothelialization is one of the effective methods to create an anti-thrombogenic surface of artificial blood vessels. In the present study, a series of biodegradable gene carriers, namely MPs/pEGFP-ZNF580 complexes, with core/shell structure and low toxicity were prepared, ZNF580 gene was carried into ECs by these complexes.

With great interest, we synthesized the amphiphilic triblock copolymers from mPEG, MMD, L-LA, and/or GA and PEI. Using hydrophilic mPEG as the initiator, three kinds of diblock copolymers were prepared via ROP. After the graft of PEI, amphiphilic triblock copolymers were obtained finally. Herein, the MMD and GA were used to adjust the degradation of the copolymer.

Morpholine-2,5-dione derivatives are a class of depsipeptide monomers which have been used to synthesize biodegradable copolymers with alternating amido and ester groups [44,45]. In the previous research, it was found that ester bonds could be hydrolyzed easily *in vitro*, while the amide bonds were relative stable [46]. However, amide bonds are hydrolyzed under enzyme catalysis *in vivo*. The amide groups improved the hydrophilicity of the materials and resulted in an increase of water absorption during degradation, this lead to the erosion rate of copolymers increased with increasing of MMD content in the copolymers [47], and also increased the hydrolysis of ester bonds. Although ester bonds play a significant role in the degradation of polydepsipeptides *in vitro* than amide bonds [32], the introduction of MMD into PLLA or PLGA polyesters affected the hydrophilicity, crystallinity as well as degradation of the copolymers. Similar results were also observed for the degradation of the amphiphilic poly(depsipeptide-co-PDO)-PEG-poly(depsipeptide-co-PDO) triblock copolymers reported by us previously [33]. Compared with other reported particles, our MPs showed the advantage for the biodegradability of the cores. In particular, after the introduction of MMD into the hydrophobic segments, the degradation behavior of hydrophobic cores depended mainly on the chemical compositions and the comonomers.

Self-assembly process was the most common and convenient technique, it was employed to prepare the MPs from these triblock copolymers. Herein, the hydrophobic core of a single microparticle was contained by many hydrophobic segments of these triblock copolymers. The function of the hydrophobic core is like a cross-linking point as previously reported [48], by this way, many short PEI (Mw = 1800) and PEG (Mw = 5000) chains were linked on the surface of MPs.

The release of pEGFP-ZNF580 from these MPs/pEGFP-ZNF580 complexes could be maintained at least for 25 days, the main reason can be explained by the suitable degradation rate of hydrophobic cores. The cytotoxicity of these developed gene carrier and their MPs/pEGFP-ZNF580 complexes was very low (cell

viability >80%) even at the concentration of 100 µg/mL after 48 h. This result indicated that the cytotoxicity was decreased greatly by introducing the PEG and short PEI chains on the surface of MPs.

To achieve a reasonable transfection effect, a large amount of low molecule weight PEI chains must be connected on the surface of MPs. This is the key factor for enabling the MPs to have high transfection effect, because low molecule weight of PEI (Mw = 1800) could not condensate DNA effectively as reported before. When many chains of PEI (low molecule weight) were connected with the core of a microparticle, pEGFP-ZNF580 could be carried into ECs through these gene carriers at appropriate N/P.

Cells were transfected with the three kinds of biodegradable MPs. The western blot result indicated that the expression of ZNF580 key protein can increase to 35.74%–46.11%. Cell migration result demonstrated that the migration rate of ECs transfected by MPs/pEGFP-ZNF580 was promoted significantly. By this way, the rapid endothelialization was realized by ZNF580 gene complexed with biodegradable MPs.

5. Conclusion

In this study, we synthesized amphiphilic triblock copolymers and prepared biodegradable microparticles with core/shell structure from them. ZNF580 gene was carried into ECs by these microparticles with suitable diameter and positive charge. ZNF580 key protein was overexpressed by these microparticles. The rapid endothelialization was significantly improved by the expression of pEGFP-ZNF580 and overexpression of ZNF580 key protein. These ZNF580 gene complexed microparticles might be used to provide the rapid endothelialization on tissue engineering scaffolds and vascular grafts.

Acknowledgments

This project was supported by the National Natural Science Foundation of China, China (Grant No. 31370969, 31271016), the International Cooperation from Ministry of Science and Technology of China, China (Grant No. 2013DFG52040, 2008DFA51170), Ph.D. Programs Foundation of Ministry of Education of China, China (No. 20120032110073) and the Program of Introducing Talents of Discipline to Universities of China, China (No. B06006).

Appendix A. Supplementary data

Supplementary data related to this article can be found at <http://dx.doi.org/10.1016/j.biomaterials.2014.04.110>.

References

- [1] Virchow R. As based upon physiological and pathological histology. *Nutr Rev* 2009;47:23–5.
- [2] Verkuijlen ROF, van Dongen MHA, Stevens AAE, van Geldrop J, Bernards JPC. Surface modification of polycarbonate and polyethylene napthalate foils by UV-ozone treatment and µPlasma printing. *Appl Surf Sci* 2014;290:381–7.
- [3] Zhao H, Feng Y, Guo J. Grafting of poly(ethylene glycol) monoacrylate onto polycarbonateurethane surfaces by ultraviolet radiation grafting polymerization to control hydrophilicity. *J Appl Polym Sci* 2011;119:3717–27.
- [4] Gao B, Feng Y, Lu J, Zhang L, Zhao M, Shi C, et al. Grafting of phosphorylcholine functional groups on polycarbonate urethane surface for resisting platelet adhesion. *Mater Sci Eng C* 2013;33:2871–8.
- [5] Wang H, Feng Y, Zhao H, Lu J, Guo J, Behl M, et al. Controlled heparin release from electrospun gelatin fiber. *J Control Release* 2011;1(152 Suppl.):e28–9.
- [6] Wang H, Feng Y, Fang Z, Yuan W, Khan M. Co-electrospun blends of PU and PEG as potential biocompatible scaffolds for small-diameter vascular tissue engineering. *Mater Sci Eng C* 2012;32:2306–15.
- [7] Yuan W, Feng Y, Wang H, Yang D, Han Y, Guo J, et al. Surface modification of electrospun porous scaffolds by S-ATRP grafting poly(ethylene glycol) methacrylate for tissue engineering. *J Control Release* 2013;172:e142–3.

- [8] Lin Q, Ding X, Qiu F, Song X, Fu G, Ji J. In situ endothelialization of intravascular stents coated with an anti-CD34 antibody functionalized heparin-collagen multilayer. *Biomaterials* 2010;31:4017–25.
- [9] Zhu Y, Gao C, He T, Shen J. Endothelium regeneration on luminal surface of polyurethane vascular scaffold modified with diamine and covalently grafted with gelatin. *Biomaterials* 2004;25:423–30.
- [10] Yang J, Zeng Y, Zhang C, Chen YX, Yang Z, Li Y, et al. The prevention of restenosis in vivo with a VEGF gene and paclitaxel co-eluting stent. *Biomaterials* 2013;34:1635–43.
- [11] Zhang H, Jia X, Han F, Zhao J, Zhao Y, Fan Y, et al. Dual-delivery of VEGF and PDGF by double-layered electrospun membranes for blood vessel regeneration. *Biomaterials* 2013;34:2202–12.
- [12] Ren D, Wang H, Liu J, Zhang M, Zhang W. ROS-induced ZNF580 expression: a key role for H₂O₂/NF- κ B signaling pathway in vascular endothelial inflammation. *Mol Cell Biochem* 2012;359:183–91.
- [13] Sun HY, Wei SP, Xu RC, Xu PX, Zhang WC. Sphingosine-1-phosphate induces human endothelial VEGF and MMP-2 production via transcription factor ZNF580: novel insights into angiogenesis. *Biochem Biophys Res Commun* 2010;395:361–6.
- [14] Ratanajanchai M, Lee DH, Sunintaboon P, Yang SG. Photo-cured PMMA/PEI core/shell nanoparticles surface-modified with Gd-DTPA for T1 MR imaging. *J Colloid Interface Sci* 2014;415:70–6.
- [15] Liu Z, Zhang Z, Zhou C, Jiao Y. Hydrophobic modifications of cationic polymers for gene delivery. *Prog Polym Sci* 2010;35:1144–62.
- [16] Sun J, Zeng F, Jian H, Wu S. Conjugation with betaine: a facile and effective approach to significant improvement of gene delivery properties of PEI. *Biomacromolecules* 2013;14:728–36.
- [17] Godbey WT, Wu KK, Mikos AG. Size matters: molecular weight affects the efficiency of poly(ethylenimine) as a gene delivery vehicle. *J Biomed Mater Res* 1999;45:268–75.
- [18] Zhang Z, Yang C, Duan Y, Wang Y, Liu J, Wang L, et al. Poly(ethylene glycol) analogs grafted with low molecular weight poly(ethylene imine) as non-viral gene vectors. *Acta Biomater* 2010;6:2650–7.
- [19] Zhang Z, Ni J, Chen L, Yu L, Xu J, Ding J. Biodegradable and thermoreversible PCL-PEG-PCL hydrogel as a barrier for prevention of post-operative adhesion. *Biomaterials* 2011;32:4725–36.
- [20] Feng Y, Chen C, Zhang L, Tian H, Yuan W. Synthesis and characterization of novel copolymers based on 3(S)-methyl-morpholine-2,5-dione. *Trans Tianjin Univ* 2012;18:315–9.
- [21] Zhao Y, Li J, Yu H, Wang G, Liu W. Synthesis and characterization of a novel polydepsipeptide contained tri-block copolymer (mPEG-PLLA-PMMD) as self-assembly micelle delivery system for paclitaxel. *Int J Pharm* 2012;430:282–91.
- [22] Jeon O, Lee SH, Kim SH, Lee YM, Kim YH. Synthesis and characterization of poly(l-lactide)-poly(ϵ -caprolactone) multiblock copolymers. *Macromolecules* 2003;36:5585–92.
- [23] Chen CJ, Wang JC, Zhao EY, Gao LY, Feng Q, Liu XY, et al. Self-assembly cationic nanoparticles based on cholesterol-grafted bioreducible poly(amidoamine) for siRNA delivery. *Biomaterials* 2013;34:5303–16.
- [24] Gargouri M, Sapin A, Arica Yegin B, Merlin JL, Becuwe P, Maincent P. Photochemical internalization for pDNA transfection: evaluation of poly(D,L-lactide-co-glycolide) and poly(ethylenimine) nanoparticles. *Int J Pharm* 2011;403:276–84.
- [25] Cheng Q, Huang Y, Zheng H, Wei T, Zheng S, Huo S, et al. The effect of guanidinylation of PEGylated poly(2-aminoethyl methacrylate) on the systemic delivery of siRNA. *Biomaterials* 2013;34:3120–31.
- [26] Zubair M, Ekholm A, Nybom H, Renvert S, Widen C, Rumpunen K. Effects of *Plantago major* L. leaf extracts on oral epithelial cells in a scratch assay. *J Ethnopharmacol* 2012;141:825–30.
- [27] Hung WC, Chang HC. Indole-3-carbinol inhibits Sp1-induced matrix metalloproteinase-2 expression to attenuate migration and invasion of breast cancer cells. *J Agric Food Chem* 2009;57:76–82.
- [28] Wu J, Mao Z, Gao C. Controlling the migration behaviors of vascular smooth muscle cells by methoxy poly(ethylene glycol) brushes of different molecular weight and density. *Biomaterials* 2012;33:810–20.
- [29] Frisman I, Seliktar D, Bianco-Peled H. Nanostructuring of PEG-fibrinogen polymeric scaffolds. *Acta Biomater* 2010;6:2518–24.
- [30] Li X, Kong X, Shi S, Gu Y, Yang L, Guo G, et al. Biodegradable MPEG-g-Chitosan and methoxy poly(ethylene glycol)-b-poly(ϵ -caprolactone) composite films: Part 1. Preparation and characterization. *Carbohydr Polym* 2010;79:429–36.
- [31] Şen Karaman D, Gulin-Sarfrız T, Hedström G, Duchanoy A, Eklund P, Rosenholm JM. Rational evaluation of the utilization of PEG-PEI copolymers for the facilitation of silica nanoparticle systems in biomedical applications. *J Colloid Interf Sci* 2014;418:300–10.
- [32] Feng Y, Lu J, Behl M, Lendlein A. Progress in deipeptide-based biomaterials. *Macromol Biosci* 2010;10:1008–21.
- [33] Zhang L, Feng Y, Tian H, Shi C, Zhao M, Guo J. Controlled release of doxorubicin from amphiphilic deipeptide-PDO-PEG-based copolymer nanosized microspheres. *React Funct Polym* 2013;73:1281–9.
- [34] Burt HM, Zhang X, Toleikis P, Embree L, Hunter WL. Development of copolymers of poly(D,L-Lactide) and methoxypolyethylene glycol as micellar carriers of paclitaxel. *Colloid Surf B* 1999;16:161–71.
- [35] Merdan T, Kunath K, Petersen H, Bakowsky U, Voigt KH, Kopecek J, et al. PEGylation of poly(ethylene imine) affects stability of complexes with plasmid DNA under in vivo conditions in a dose-dependent manner after intravenous injection into mice. *Bioconjug Chem* 2005;16:785–92.
- [36] Guo S, Huang Y, Wei T, Zhang W, Wang W, Lin D, et al. Amphiphilic and biodegradable methoxy polyethylene glycol-block-(polycaprolactone-graft-poly(2-(dimethylamino)ethyl methacrylate)) as an effective gene carrier. *Biomaterials* 2011;32:879–89.
- [37] Zhao F, Yin H, Li J. Supramolecular self-assembly forming a multifunctional synergistic system for targeted co-delivery of gene and drug. *Biomaterials* 2014;35:1050–62.
- [38] Yang J, Zhang P, Tang L, Sun P, Liu W, Zuo A, et al. Temperature-tuned DNA condensation and gene transfection by PEI-g-(PMEOMA-b-PHEMA) copolymer-based nonviral vectors. *Biomaterials* 2010;31:144–55.
- [39] Arote R, Kim TH, Kim YK, Hwang SK, Jiang HL, Song HH, et al. A biodegradable poly(ester amine) based on polycaprolactone and polyethylenimine as a gene carrier. *Biomaterials* 2007;28:735–44.
- [40] Elfinger M, Pfeifer C, Uezguen S, Golas MM, Sander B, Maucksch C, et al. Self-assembly of ternary insulin-polyethylenimine (PEI)-DNA nanoparticles for enhanced gene delivery and expression in alveolar epithelial cells. *Biomacromolecules* 2009;10:2912–20.
- [41] Jorge AF, Dias RS, Pereira JC, Pais AACC. DNA condensation by pH-responsive polycations. *Biomacromolecules* 2010;11:2399–406.
- [42] Kunath K. Low-molecular-weight polyethylenimine as a non-viral vector for DNA delivery: comparison of physicochemical properties, transfection efficiency and in vivo distribution with high-molecular-weight polyethylenimine. *J Control Release* 2003;89:113–25.
- [43] Hägglund B, Sandberg G. Effect of L-alanine and some other amino acids on thymocyte proliferation in vivo. *Immunobiology* 1993;188:62–9.
- [44] Feng Y, Guo J. Biodegradable polydepsipeptides. *Int J Mol Sci* 2009;10:589–615.
- [45] Abayasinghe NK, Perera KPU, Thomas C, Daly A, Suresh S, Burg K, et al. Amido-modified polylactide for potential tissue engineering applications. *J Biomat Sci-Polym E* 2004;15:595–606.
- [46] Helder J, Dijkstra PJ, Feijen J. In vitro degradation of glycine/DL-lactic acid copolymers. *J Biomed Mater Res* 1990;24:1005–20.
- [47] Du F, Ye W, Gu Z, Yang J. Synthesis and in vitro degradation of copolymers of glycolide and 6 (R,S)-methylmorpholine-2,5-dione. *J Appl Polym Sci* 1997;63:643–50.
- [48] Yuk SH, Oh KS, Cho SH, Lee BS, Kim SY, Kwak B-K, et al. Glycol chitosan/heparin immobilized iron oxide nanoparticles with a tumor-targeting characteristic for magnetic resonance imaging. *Biomacromolecules* 2011;12:2335–43.